JREE: Vol. 12, No. 4, (Autumn 2025) 53-63

Journal of Renewable Energy and Environment

Journal Homepage: www.jree.ir

Materials and Energy Research Center

MERC

Research Note

# A Novel 3D-Printed Turbine to Harvest Renewable Energy from Water Pipeline System for Street Lighting

Ching Yee Yong*, Joshua Zhong Zhi Wong

*Centre for Research of Innovation & Sustainable Development, School of Engineering and Technology, University of Technology Sarawak, No. 1, Jalan Universiti, 96000, Sibu, Sarawak, Malaysia.*

*PAPER INFO*

*Paper history:*
Received: 13 January 2025
Revised: 11 July 2025
Accepted: 22 September 2025

*Keywords*:
Renewable Energy,
Clean Energy,
Turbine,
Water Pipeline,
Flow Rate

*ABSTRACT*

Pressure control valves are commonly employed in water distribution systems because excessive water pressure can cause significant damage to infrastructure. As an alternative, a turbine can serve a dual purpose by ensuring that the pressure drop across the turbine matches the required pressure drop, while simultaneously transferring a portion of the surplus energy to the turbine. This energy is then converted into electricity through a connected generator. The objective of this research is to design a turbine that can be integrated into pipelines to harness energy from flowing water and generate electricity. A spherical cross-flow turbine was selected for this system because it can sweep the maximum area of the pipe cross-section. Owing to its compact structure and simple mechanics, the spherical design is well-suited for use in urban pipeline networks to enable decentralized renewable energy production. To evaluate performance, turbines with varying parameters were designed and fabricated using 3D printing. Experimental results show that a turbine with six blades set at an angle of 35° achieved the highest output power of 0.231 W. The findings indicate that increasing the number of blades, enlarging the turbine diameter, and adopting a greater angle of attack lead to higher output power. The maximum efficiency achieved by the proposed turbine was 70.64%. Furthermore, the estimated theoretical output power was calculated as 207 W, which is sufficient to supply electricity to street lighting or other nearby loads. In conclusion, this research demonstrates that clean energy can be generated by installing a compact turbine within a pipeline system. The proposed spherical cross-flow turbine offers a portable, cost-effective, and flexible solution for decentralized renewable energy applications.

https://doi.org/10.30501/jree.2025.498040.2222

## 1. INTRODUCTION

High water pressure, especially in urban areas, is essential to ensure that water can be delivered to consumers throughout the distribution system (Ghorbanian et al., 2016; Hangan et al., 2022). However, excessive pressure must be reduced to prevent damage to the pipeline system and avoid excessively high water pressure at the consumer's end (Jilani & Razali, 2018; Bideris-Davos & Vovos, 2023). For this reason, water valves are commonly used in pipeline systems to lower the pressure to an acceptable level before distribution to households. Instead of conventional reducing valves, a turbine connected to a generator can be employed to achieve pressure reduction while simultaneously producing clean energy (Coronado-Hernández et al., 2017).

In this setup, the flow of water along the pipeline acts as the driving force, converting kinetic energy into renewable and cost-free electricity (Das et al., 2021). Existing turbine designs, such as those developed by Gorlov and Lucid, face limitations. Their inefficiency under low-flow conditions has been documented (Ham et al., 2024), and their mechanical complexity and high fabrication costs restrict deployment in confined environments such as urban pipeline networks.

The rounded cross-flow turbine offers a potential solution (Anand et al., 2021), as its simplified blade geometry enables fabrication through 3D printing. It is also easy to operate, cost-effective, and practical to implement. This study aims to design an environmentally friendly, 3D-printed turbine capable of harvesting energy from water flow within pipelines. The scope of the work is restricted to a lab-scale prototype for pilot testing. The turbine was designed with a spherical geometry, emphasizing portability, ease of installation, and straightforward disassembly.

## 2. RESEARCH REVIEW

### 2.1. Case Study

In this study, a horizontal cross-flow turbine for a hydro-harvesting system was designed. The turbine consists of eight blades, a top and bottom plate, and a shaft. The blades are welded to the top and bottom plates, which are connected to the shaft. A bearing was mounted on the shaft to accommodate radial and axial loads, while a DC generator was coupled to the shaft for power generation. An air blower was used to evaluate turbine efficiency instead of water flow, output voltage and current were measured with a digital multimeter (Ong, 2011).

*Corresponding Author's Email: chingyee@uts.edu.my (C. Y. Yong)
URL: https://www.jree.ir/article_230955.html

Please cite this article as: Yong, C. Y. & Wong, J. Z. Z. (2025). A Novel 3D-Printed Turbine to Harvest Renewable Energy from Water Pipeline System for Street Lighting. *Journal of Renewable Energy and Environment (JREE)*, 12(4), 53-63. https://doi.org/10.30501/jree.2025.498040.2222

SolidWorks software was employed to design the turbine configuration. A stainless-steel hollow shaft was selected due to its ability to withstand high water pressure. To support the four turbine blades, a square aluminium hollow structure was added around the shaft. This design incorporated two gear sizes to enhance the generator's rotational speed. Performance testing was conducted using a high-pressure water jet directed into a tank containing the turbine, as well as by placing the turbine directly in a river. Results showed that the turbine exposed to the high-pressure water jet produced greater power compared to operation in river flow, indicating that water pressure strongly influences turbine performance (Abd Rahman & Syazwani, 2012).

The Gorlov helical (cross-flow) turbine, in contrast, was developed to operate under ultra-low head conditions (Etemadeasl et al., 2024). The objective of this research was to determine the parameters of an ultra-low head hydraulic turbine for a hydroelectric generation system designed to maximize stream flow energy in the Way Tebu irrigation canal at Banjar Agung Udik Village. Parameters calculated included turbine diameter, height, number of blades, rotor shape, and blade angle. The selected configuration employed three blades, with a turbine height of 1 m, a diameter of 2 m, and a blade inclination angle of 62°. Airfoil-shaped blades were considered due to their ability to enhance performance by generating pressure differences on either side of the blade, thus inducing rotation through lift and drag forces. Various airfoils were tested to compare efficiency. The system comprised a helical rotor, belt pulley, and a generator.

The turbine was installed in a river, where water flow provided the driving kinetic energy. The rotor turned the pulley, which in turn drove the generator to produce electricity. Findings indicated that airfoil blades improved turbine efficiency, with the NACA0030 airfoil achieving the highest efficiency at 33.78% (Sinaga et al., 2018).

To evaluate turbine performance, a Savonius turbine (vertical-axis turbine) with varying blade numbers was designed and fabricated using a 3D printer. The turbine was constructed from Polylactic Acid (PLA) with a thickness of 2 mm. The experimental setup involved pumping water from a lower reservoir to an upper reservoir, after which the water was released to flow through the turbine. Results showed that the three-bladed turbine generated higher power compared to the two-bladed design. However, as the number of blades increased from four to six, the power output decreased. The superior performance of the three-bladed turbine was attributed to the optimal interaction between water flow and the turbine's rotational speed. The spacing between blades allowed water to flow more naturally through the gaps, striking other sections of the turbine. This effect enhanced the positive thrust force while reducing the opposing centrifugal force. In contrast, increasing the number of blades raised drag forces, which reduced rotational speed and, consequently, power output. The study also investigated four different flow rate variations to assess their effect on turbine performance. Results indicated that higher flow rates produced greater power output. Overall, turbine performance was strongly influenced by both the number of blades and the water flow rate (Hamzah et al., 2018).

The efficiencies of the Lucid Spherical Turbine (LST) and the Gorlov Helical Turbine (GHT) were evaluated in open water rather than within a pipe of equal dimensions. Structurally and in scale, both turbines are comparable. However, the GHT is primarily designed for open-water applications (preferably at flow rates greater than 1.5 m/s), whereas the LST is intended for confined circular pipes or conduits. Consequently, the peak kinetic energy capture of the LST is 35%, compared to 46% for the GHT. This indicates that in a tank environment, the LST is less effective than the GHT in harnessing hydrokinetic energy. The maximum power coefficient of the LST is 21%, while that of the GHT is 28%. Therefore, LST turbines are better suited for pipeline applications (Bachant & Wosnik, 2015).

This study also addresses the objective of developing a turbine capable of generating high torque while operating under low-pressure conditions. Three types of cross-flow turbines were considered as suitable for integration into pipelines: Lucid, Darrieus, and Gorlov turbines. The effect of twisted angles on different airfoil types was investigated to determine optimal turbine efficiency. Findings revealed that the Lucid turbine equipped with a NACA0018 airfoil and a 120° twist angle generated the highest torque and pressure loss. When shaped spherically, the Lucid turbine produced the greatest power output due to the increased swept area of its blades. Comparatively, the 10° twisted Gorlov turbine with a NACA0015 airfoil produced 31.3% less torque and 51.4% less pressure loss than the Lucid turbine, while the 20° twisted Gorlov turbine with the same airfoil design achieved 4.7% less torque and 49.3% less pressure loss. As a result, the 20° twisted Gorlov turbine was recommended for the turbo-solenoid method, as it provided reduced pressure loss compared to the Lucid turbine. Additionally, the Darrieus turbine with a NACA0015 profile exhibited 9% greater torque but 1.4% higher pressure loss than its NACA0018 counterpart. These results confirm that both airfoil profile and twist angle significantly affect turbine torque and pressure loss (Mutlu & Çakan, 2018).

An experimental study was also conducted to investigate the impact of converging pipes on turbine performance. The test pipe section had a length of $Lo = 2 \times L = 2$ m and a diameter of $Do = 1.8$ m, featuring an inlet converging section. A four-bladed spherical rotor was positioned at the midpoint of the converging pipe. The rotor employed a NACA0020 airfoil, with a chord length of 140 mm, a height of 0.97 m, a diameter of 1.14 m, and a blade overlap of $e = 2$. Both the converging section and the turbine were installed at the pipe's midpoint. The results demonstrated that the maximum rotor power coefficient without the converging pipe was 0.204, while with the converging pipe, it increased to 0.224 (Mosbahi et al., 2019).

With its distinctive design, the Gorlov Helical Turbine (GHT) has garnered attention as a promising option for hydrokinetic power generation. While extensive research has been conducted to evaluate its capabilities and limitations under different operating conditions, Rendi et al. (2024), for example, demonstrated that the GHT outperforms classical turbines in terms of efficiency. However, its performance diminishes at low water velocities, as the GHT relies solely on lift forces. To address this limitation, modifications to the blade design that incorporate drag forces have been proposed to enhance performance under such conditions. Conversely, Espina-Valdés et al. (2022) reported that the GHT produced higher mechanical power than the Darrieus-type turbine at low current velocities, achieving power coefficients greater than 1. This finding suggests that the helical blade configuration may offer distinct advantages in certain low-flow environments. Nevertheless, a study by University of Aberdeen (2023) questioned the GHT's viability at low Reynolds numbers, noting its inability to generate positive torque under such

conditions. This highlights that, while the GHT has potential, its optimal operating range may be narrower than initially anticipated. Further research by Pranio and Karnowo (2019) emphasized that the GHT's efficiency is strongly influenced by both blade number and water velocity, with each parameter requiring careful optimization. Collectively, these findings suggest that although the GHT is a promising alternative to conventional turbines, its deployment must be carefully tailored to environmental conditions and design choices. Continued research is therefore essential for the broader realization of hydrokinetic energy's potential.

The review has also been extended to critically assess the performance limitations of both Gorlov and Savonius turbines (Kirke, 2024). In this context, the spherical cross-flow turbine was particularly highlighted for its suitability in constrained environments such as urban pipelines, where it demonstrates high operational efficiency. Moreover, recent investigations into steady-state hydrokinetic flow (Ibrahim et al., 2025) further underline the efficiency advantages of spherical collector designs under stable flow conditions—a scenario particularly relevant to practical applications.

Table 1 summarizes the critical review across key aspects of the Gorlov, Savonius, and Lucid turbines. For small-scale, low-cost applications, a Savonius turbine is the most economical option for a 4-inch diameter configuration. However, Gorlov or Lucid turbines, while more expensive, offer superior efficiency and may be better suited to higher-performance applications. Table 2 presents the cost analysis of conventional turbines. A novel approach to transferred hydropower generation is the integration of 3D-printed turbines into existing pipeline networks, directly addressing the high costs and logistical challenges associated with traditional turbine systems.

Additive manufacturing enables substantial reductions in both production and installation expenses, contrasting sharply with conventional installations that require heavy machinery, extensive civil works, and significant upfront capital investment.

By allowing turbines to be retrofitted into current infrastructure, this method eliminates costly land-use approvals and reduces the need for extensive environmental impact assessments—two major contributors to project expenses and delays. Moreover, the in-pipe configuration and modular design simplify maintenance and operation. Standardized, easily replaceable components take the place of expensive, highly specialized parts and labor traditionally required for Kaplan, Francis, or Pelton turbines.

This approach not only creates a viable model for distributed energy generation but also mitigates both the initial and lifecycle costs, thereby improving the overall economic feasibility of small-scale hydropower projects.

### 2.2. Innovative Proposed Design with Generator

In this paper, a bipolar stepper motor with four wires is employed as a generator to produce electrical energy. The motor's output is rectified using a rectifier circuit, and the voltage is further increased through a voltage doubler circuit composed of a few key components: an LED, a diode, a Zener diode, a rechargeable battery, and a capacitor.

The two outputs of the voltage doubler circuit are connected in series to achieve a higher DC voltage. When connected directly to the doubler circuit's output through a 3.3 kΩ resistor, the system is capable of powering nine LEDs. Additionally, the rechargeable battery can be charged efficiently by continuously monitoring its voltage level.

**Table 1.** Comparison between Gorlov, Savonius, and Lucid turbines. (Awandu et al., 2022; Aziz et al., 2021; Hwang & Kim, 2024; Itani et al., 2020; Jayaram & Bavanish, 2022; Kamal & Saini, 2022; Kamoji et al., 2009; Mosbahi et al., 2022; Reddy et al., 2022; Roy & Saha, 2015; Saini & Saini, 2023; Shankara et al., 2024; Vijayan & Retnam, 2022)

| Aspect | Gorlov | Savonius | Lucid |
|---|---|---|---|
| Efficiency | Moderate<br>Suffers from low tip-speed ratios (TSR), which reduces aerodynamic performance. | Low<br>Typical power coefficient (Cp) ranges from 0.05 to 0.30. | High<br>Effective in low-flow conditions, but performance decreases in high-flow environments. |
| Self-starting | Yes<br>Good self-starting behaviour due to helical blade geometry. | Yes<br>It starts easily, even at low wind speeds. | Outstanding performance at low speeds. |
| Directional sensitivity | Omnidirectional<br>There is no need for a yaw mechanism. | Omnidirectional<br>Functions effectively with wind from any direction. | High adaptability to changing flow directions. |
| Torque characteristics | Consistent torque output due to uninterrupted blade exposure. | High torque ripple caused by negative torque on | High torque under low-speed conditions. |
| Structural complexity | High-precision helical blade fabrication is required. | Low<br>Simple construction and assembly. | Straightforward and easy to maintain. |
| Performance in low-flow | Moderate<br>It performs better than Darrieus in water flows but is limited in ultra-low flow rates. | High<br>Excellent at capturing wind energy in low-speed environments. | Optimized and highly efficient. |
| Scalability | Moderate to high suitability for tidal and hydrokinetic arrays. | Limited to small-scale applications because of low efficiency. | Moderate with potential for small to medium-scale projects. |
| Maintenance requirements | Moderate<br>Requires regular inspection of blade integrity. | Low<br>The minimal number of moving parts makes it easy to maintain. | Low<br>It consists of fewer components and more straightforward mechanics. |
| Design optimization needs | It requires aerodynamic and structural optimization to reduce drag and increase the coefficient of performance (Cp). | Sensitivity to rotor shape, overlap ratio, and blade aspect ratio for improving efficiency. | There remains room for improvement, especially for larger installations. |
| Cost for small-scale | USD 500-2000 | USD 100-400 | USD 1500-5000 |

**Table 2.** Cost analysis of the conventional turbines.

| Category | Findings | Reference | Cost Impact |
|---|---|---|---|
| **Capital investment** | High up front for installation, infrastructure, and civil works. The price of turbine parts includes mechanical, hydraulic, and electrical parts. Prices depend on the type of turbine (Gorlov, Savonius, Kaplan, Francis, Pelton, or Lucid). | Kumar & Saini, 2022; Khalid et al., 2023 | High (up to 70% of the total project cost) |
| **Maintenance and operation** | Regular maintenance, like checking and lubricating. The costs of running the business over time include replacing turbine parts. It requires less maintenance than other methods of generating power. | Whitby, 2021; Yazdi, 2024 | Medium (10-15% annually) |
| **Energy production efficiency** | Very dependent on the type of turbine and the water flow. The efficiency of energy generation depends on the state of the water. Better designs for turbines can help lower costs. | Rahman, 2022; Mamassis et al., 2021 | High (directly affects the payback period) |
| **Environmental impact and regulatory compliance** | Costs associated with obtaining environmental impact assessments, land use approvals, and regulatory clearances. Some areas provide financial incentives to businesses that comply with environmental regulations. | Rahman, 2022; Strielkowski et al., 2021 | Medium (varies by region) |
| **Lifecycle costs and return on investment (ROI)** | The full cost of the turbine's life cycle is usually 20 years. The time it takes to repay the loan ranges from 7 to 15 years, depending on the energy price and the turbine's efficiency. | Walker & Thies, 2022; Skroufouta & Baltas, 2021; Tu et al., 2023 | Medium to high (depends on site-specific conditions) |
| **Decommissioning costs** | Taking down the infrastructure after the turbine's useful life is over. Saving money by reusing parts. | Quaranta & Davies, 2022; Musa et al., 2023 | Low to medium (depends on site) |

## 3. METHODOLOGY

The design flow is illustrated in Figure 1. Initially, water was pumped into the pipe at a flow rate of 200 L/min using a water pump. The pipe diameter was set to 4 inches, and the turbine had an approximate diameter of 10 cm. As water flows through the pipe, it possesses significant energy in both kinetic and pressure forms. The flowing water then strikes the spherical blades of the turbine, causing it to rotate. A vertical shaft was positioned at the center of the turbine and coupled to the stepper motor, which functions as a generator. Consequently, as the shaft rotates with the turbine, the generator rotor also spins, cutting magnetic flux lines and inducing an electromotive force (EMF) in the conductors (Altgilbers et al., 2000; Ehya & Faiz, 2022). This EMF generates a current when the circuit is closed. The magnitude of the EMF is proportional to the rate at which the flux is cut, meaning that higher shaft rotation results in greater energy generation (Miao et al., 2022). The stepper motor, as an electrical machine, converts the mechanical energy from the turbine into electrical energy. The generator output, initially in AC, is passed through a rectifier circuit to convert it to DC, which is then transmitted to the load and measured.

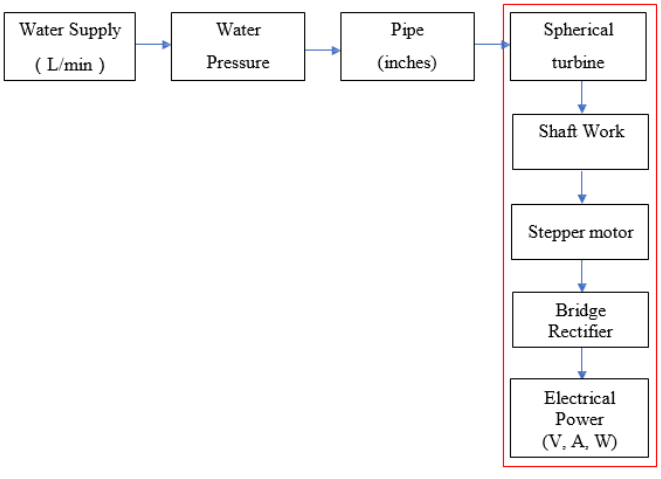


**Figure 1.** Block diagram of the research.

### 3.1. Related Calculation

The electrical power of the turbine can be estimated through the calculation below (Williams, 2003):

$$P_t = \rho \times g \times nt \times H_n \times Q \quad (1)$$

where ρ is the density of water, g is the acceleration due to Earth's gravity, equal to 9.81 $m^2/s$, $nt$ is turbine efficiency, $H_n$ is the net head and $Q$ is the water flow rate equation in cubic meters per second ($m^3/s$). The torque generated can be calculated by using the equation below, where τ is torque and ω is angular speed:

$$P = \tau \times \omega \quad (2)$$

### 3.2. Proposed Turbine Design

In this study, a spherical turbine was proposed. Although cylindrical Darrieus and Gorlov turbines generally exhibit higher performance than spherical turbines (Singh & Singal, 2017), the spherical design offers advantages in compactness and ease of installation. The turbine consists of several key components, including blades, a central shaft, top and bottom plates. The proposed turbine is equipped with five blades. To construct the spherical turbine, the top and bottom plates are circular, and the turbine blades are arranged along a circular line on the surface of the sphere. A shaft is inserted at the center of the turbine to enhance structural stability.

The height of the blades determines the region of the spherical turbine that contributes to electricity generation and affects the turbine's effective swept area. Given the spherical shape, the blade height equals the turbine's diameter. During construction, the height should be optimized to maximize the blade's swept area and enhance energy harvesting efficiency (Howey et al., 2011; Umar et al., 2022). The turbine's initial diameter is approximately 10 cm.

In this design, airfoil-shaped blades are used. As fluid flows over the blades, lift forces are generated, causing the turbine to rotate more rapidly. The turbine's performance is significantly influenced by the angle of attack, which optimizes lift forces and minimizes drag forces throughout a complete rotation. The

angle of attack is defined by the orientation of the chord line relative to the fluid flow direction. In this design, the initial angle of attack is set to 15° (Yavuz & Koç, 2012).

Increasing the number of airfoils in each cross-sectional plane, corresponding to more blades, increases the total lift and drag forces acting on the turbine, thereby enhancing rotational speed (Siavash et al., 2020). For this design, the turbine is initially equipped with five blades.

## 4. THE PROPOSED DESIGN AND PROTOTYPE

Two turbine designs are proposed for testing. The first design, described above, features five blades, a 20° angle of attack, a 10 cm turbine diameter, a 0.5 cm blade width, and a 2 cm blade length. According to McCroskey, the resultant force on a blade increases with a higher angle of attack; therefore, multiple attack angles will be evaluated to determine optimal turbine performance. Initial tests indicate that a five-blade configuration generates more energy than a three-blade configuration. Additionally, a six-blade turbine will be tested. The best-performing configuration will be selected based on these tests. Subsequently, the performance of the turbine will be assessed using the second proposed design.

### 4.1. First Proposed Design of Turbine

Fusion 360, developed by Autodesk and powered by the cloud, is a versatile 3D design and engineering software widely used for product design, mechanical engineering, and simulations. This platform integrates CAD (Computer-Aided Design), CAM (Computer-Aided Manufacturing), and CAE (Computer-Aided Engineering) tools, allowing users to design, simulate, and prototype within a single workstation. Fusion 360 supports parametric, direct, and freeform modeling methods, providing flexibility to meet a wide range of design and manufacturing needs. Its cloud-based functionality enables seamless collaboration, allowing team members to work remotely with real-time design updates. Additionally, the software offers advanced simulation capabilities, including stress, thermal, and motion analyses, which are valuable for optimizing designs prior to physical prototyping (Timmis, 2021).

### 4.2. Second Proposed Design of Turbine

For this design, the turbine diameter is set at 5 cm. Two turbines will be mounted on a single shaft inside a 10 cm pipe, as illustrated in Figure 3. The number of blades and the attack angle are selected based on the optimal performance observed in the first proposed design.

### 4.3. Cover for Turbine

Figure 4 illustrates the cover designed to hold the turbine. A hole at the top of the cover accommodates the ball bearing. Both the cover and the pipe have a diameter of 4 inches. Sealed steel bearings (SKF 6200) are used to minimize shaft friction and wear, thereby enhancing operational efficiency and longevity (Quaranta & Davies, 2022). The upper cover is 3D-printed with PLA material and sealed with rubber gaskets to prevent leakage and vibration.

### 4.4. The Turbine

Figures 5–7 illustrate the turbine with varying numbers of blades, angles of attack, and diameters, as well as the 3D-printed turbine cover. The figures also depict the different angles of attack of the blades. Figure 8 shows the installation of the turbine, shaft, and cover. First, two holes were drilled into the pipe, and the shaft was inserted through the center of the turbine and passed through the holes. Two covers with ball bearings were then used to support the shaft, ensuring smooth rotation. Finally, the covers were secured in place with screws and nuts.

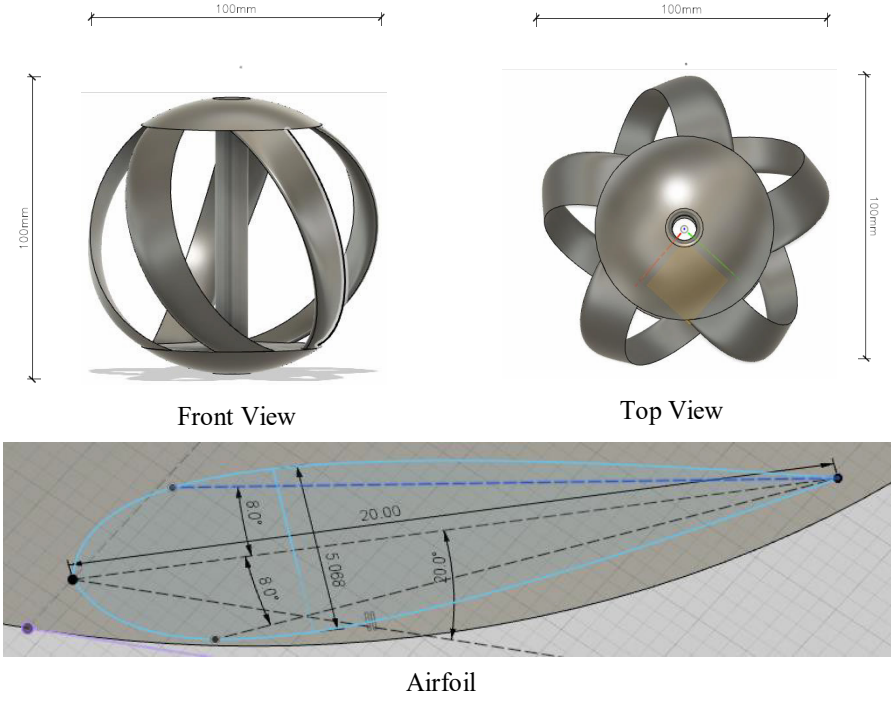


**Figure 2.** The first proposed design of the turbine.

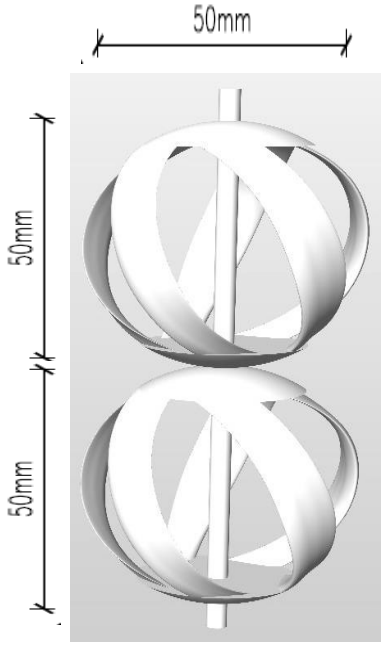


**Figure 3.** The second proposed design of the turbine.

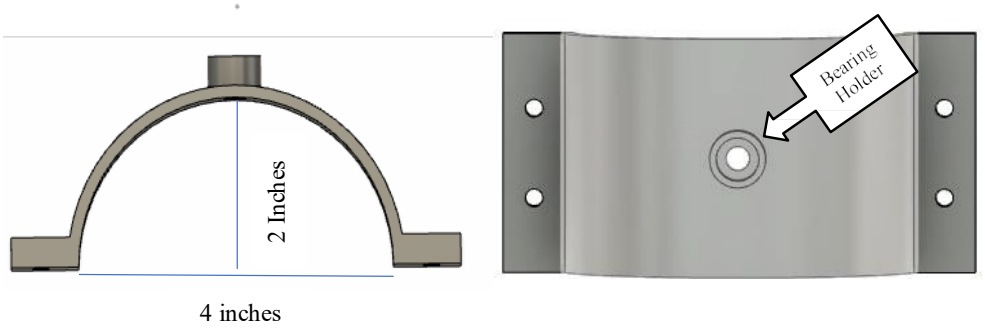


**Figure 4.** Turbine cover.

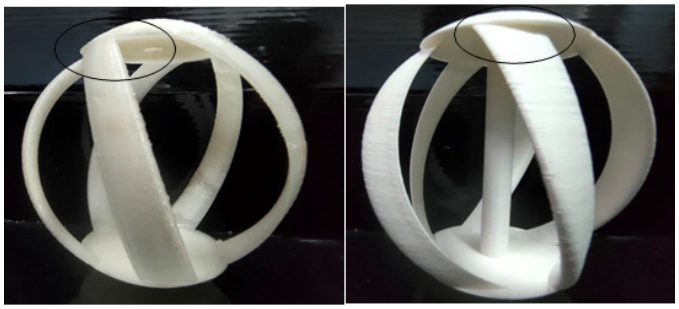

**Figure 5.** Turbine with 5 blades, 20° (left) and 35° (right).

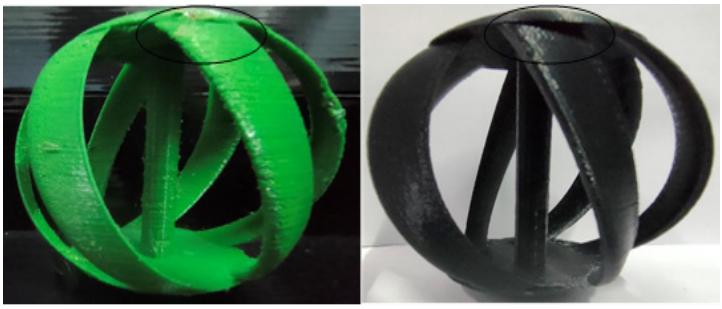

**Figure 6.** Turbine with 6 blades, 20° (left) and 35° (right).

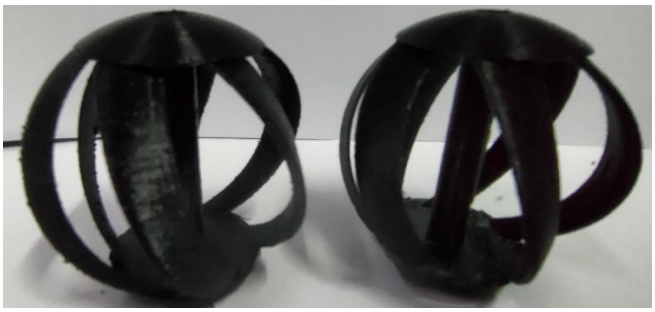

**Figure 7.** 5mm turbine with 6 blades, 35° for the second proposed design.

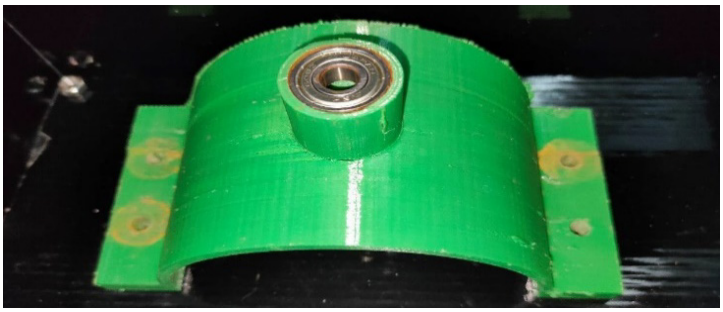

**Figure 8.** Cover for the turbine.

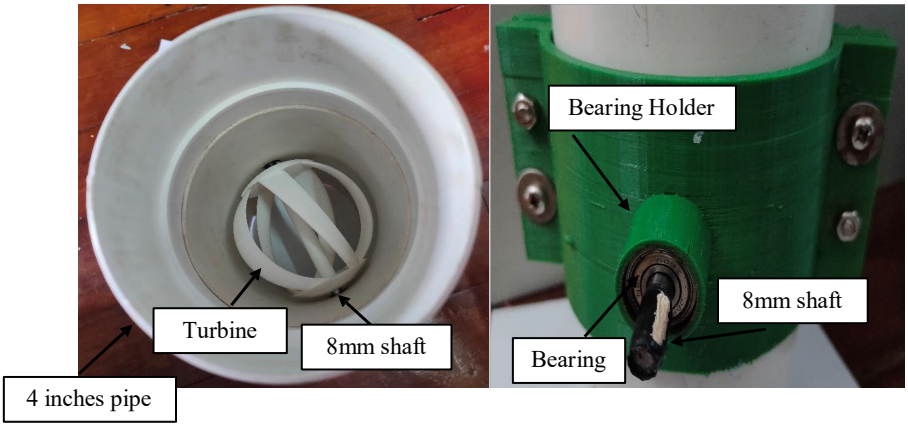


**Figure 9.** The connection between the turbine and the turbine cover.

### 4.5. Bridge Rectifier Circuit Connection

The stepper motor produces two AC input phases, designated as phase A and phase B, which are connected to the AC terminals of the rectifier. Two rectifiers are connected in series, generating a doubled output voltage. A capacitor is connected in parallel with the rectifier to smooth the DC output. The LED illuminates when the rotor of the stepper motor is rotating. When the rotor stops, the LED remains lit briefly due to the residual charge in the capacitor.

Figure 10 illustrates the circuit connection among the LCD module, Arduino Uno, and IR sensor. The IR sensor comprises two small LEDs on the board, serving as the transmitter and

receiver. When one LED lights up, it transmits IR rays. If both LEDs light up upon encountering an obstacle, it indicates that the IR receiver has received the reflected rays. Once the obstacle is removed, the receiver LED lights up again, which is considered one detection event. The Arduino Uno counts the RPM based on these events and displays the result on the LCD module, as shown in Figure 11. The IR sensor's control unit allows adjustment of the distance at which the IR rays are transmitted and received.

### 4.6. The Complete Prototype

Figure 12 illustrates the performance of the energy-harvesting system as water flows through the pipeline. The water-circulating components include tanks, pipes, and pumps. The pipeline system has a length of 120 cm and a height of 55 cm. The generator is connected to the rectifier circuit via the turbine shaft using a z-coupling for measurement purposes. Two digital multimeters were used to measure voltage and current independently. A digital tachometer sensor was positioned near the shaft, which was whitened with paint to enhance visibility, for measuring the shaft RPM. During turbine operation, readings of shaft RPM, voltage, and current were recorded. The selection of blade count (5 or 6 blades) and angles (15°, 20°, 35°) was based on previous studies (Ham et al., 2024), which identified these parameters as optimal for torque generation in low-flow hydrokinetic turbines. The net head, defined as the vertical height between the pump outlet and the turbine inlet, was approximately 0.01 m, as shown in Figure 12. Low-head turbines are typically installed in enclosed pipelines to reflect experimental conditions representative of urban pipeline environments. In such applications, particularly where water is pumped to the turbine inlet without significant elevation drop, a net head of 0.01 m is common. This choice aligns with practical urban infrastructure scenarios, where energy recovery from water flow is achievable without requiring substantial vertical height differences (Basumatary et al., 2021).

## 5. RESULT AND DISCUSSION

The results in Table 3 clearly indicate that the turbine with 6 blades and a 35° attack angle achieves the highest output power and exhibits a higher RPM compared to the other configurations. Specifically, a turbine with 6 blades generates more power than one with 5 blades, and an angle of attack of 35° produces higher output than 20°. This demonstrates that increasing the number of blades and the angle of attack enhances the turbine's performance. The turbine with 6 blades at 35° achieved the best performance and was used as a reference for testing the second proposed design.

When combining turbines, one with 6 blades at 35° and another with 5 blades at 35°, the system still performs well, but the output power decreases compared to the single turbine with 6 blades at 35°. Tests with a different DC generator showed that although the RPM was higher than that of the stepper motor, the output power was significantly lower.

Overall, the turbine with 6 blades and a 35° attack angle produces the highest output power of 0.231 W, confirming that both a higher blade count and a larger attack angle improve performance. The second proposed design, however, was unable to generate power under the tested conditions.

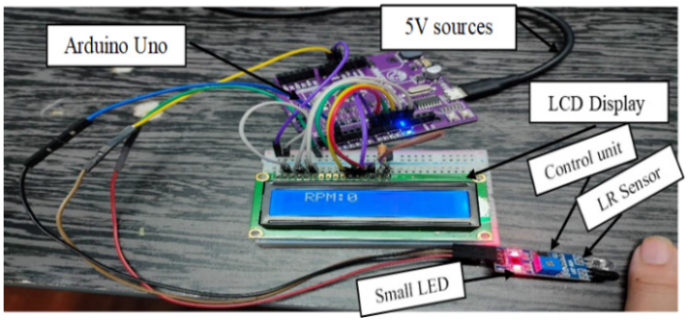


**Figure 10.** Circuit connection of a digital tachometer with an obstacle (finger).

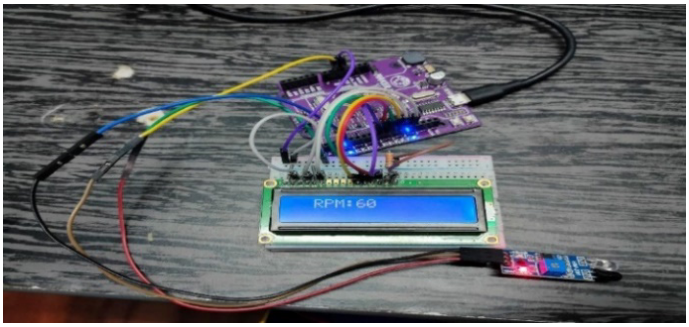


**Figure 11.** Circuit connection of the digital tachometer with RPM reading.

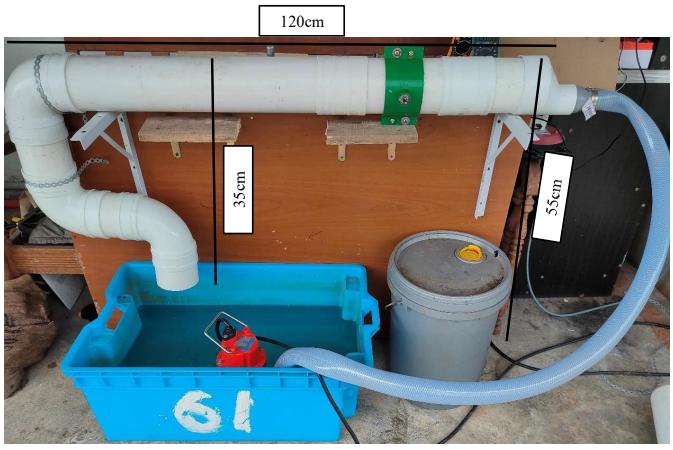


**Figure 12.** The outcome with one turbine.

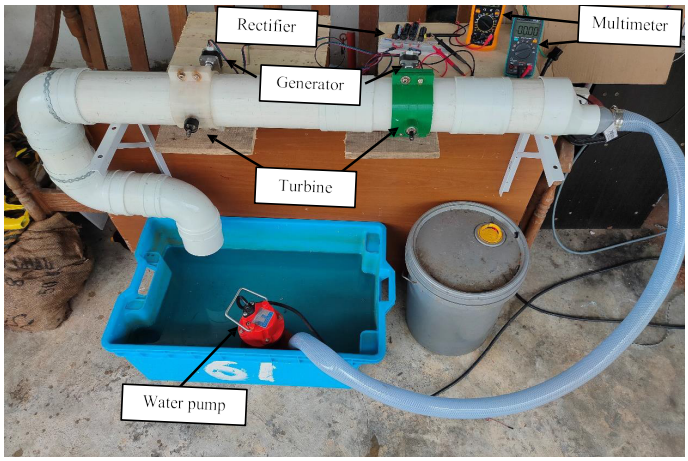


**Figure 13.** The outcome with two turbines.

**Table 3.** Data for the turbine with different attack angles and number of blades (with repeated trials).

| First Proposed Design | | | | | | | |
|---|---|---|---|---|---|---|---|
| **Trial** | **Number of blades** | **Attack angle (°)** | **Output voltage (V)** | **Output current (mA)** | **Output power (W)** | **Speed (RPM)** | **Torque (Nm)** |
| 1 | 5 | 20 | 7.69 | 17.25 | 0.133 | 239 | |
| 2 | 5 | 20 | 7.54 | 17.05 | 0.129 | 239 | |
| 3 | 5 | 20 | 7.64 | 17.16 | 0.131 | 239 | |
| Average | | | 7.62 | 17.15 | 0.131 | 239 | 0.00523 |
| Standard D. | | | 0.076 | 0.10 | 0.002 | 0 | |
| 1 | 5 | 35 | 8.85 | 20.64 | 0.183 | 299-359 | |
| 2 | 5 | 35 | 8.73 | 20.60 | 0.180 | 299-359 | |
| 3 | 5 | 35 | 8.68 | 20.40 | 0.177 | 299-359 | |
| Average | | | 8.75 | 20.55 | 0.180 | 299-359 | 0.00575 |
| Standard D. | | | 0.087 | 0.129 | 0.003 | 0 | |
| 1 | 6 | 20 | 8.31 | 19.23 | 0.160 | 299 | |
| 2 | 6 | 20 | 8.31 | 19.27 | 0.160 | 299 | |
| 3 | 6 | 20 | 8.44 | 19.47 | 0.164 | 299 | |
| Average | | | 8.35 | 19.32 | 0.161 | 299 | 0.00541 |
| Standard D. | | | 0.075 | 0.129 | 0.002 | 0 | |
| 1 | 6 | 35 | 9.75 | 23.74 | 0.229 | 359 | |
| 2 | 6 | 35 | 9.72 | 23.61 | 0.229 | 359 | |
| 3 | 6 | 35 | 9.85 | 23.71 | 0.234 | 359 | |
| Average | | | 9.76 | 23.64 | 0.231 | 359 | 0.00614 |
| Standard D. | | | 0.068 | 0.068 | 0.003 | 0 | |
| **Second Proposed Design** | | | | | | | |
| 1 | 6 | 35 | 0 | 0 | 0 | 0 | 0 |
| 2 | 6 | 35 | 0 | 0 | 0 | 0 | 0 |
| 3 | 6 | 35 | 0 | 0 | 0 | 0 | 0 |
| Average | | | 0 | 0 | 0 | 0 | 0 |
| Standard D | | | 0 | 0 | 0 | 0 | 0 |

Figure 14 presents the trial analysis of the four proposed turbine designs, including their associated error bars. A corresponding table of repeated trials and error bars is provided to illustrate the statistical variability in torque generation. The increased torque observed for the turbine with 6 blades at a 35° attack angle is explained through fluid dynamics principles, such as the lift-to-drag ratio and the effective swept area (Ibrahim et al., 2025).

The torque enhancement arises from a larger swept area, which captures more flow energy, combined with the optimal blade angle of attack (35°) that balances the forces acting on the blades. The deviation in the measured voltage ranges from 0.068 to 0.087 V (0.70–1.00%), while the deviation in the measured current varies from 0.068 to 0.129 mA (0.29–0.67%). As a result, the calculated power deviation lies between 0.002 and 0.003 W (1.25–1.67%). Since all deviations are below 2%, additional trials are deemed unnecessary. Table 4 also presents the performance of the turbine when coupled with a different DC generator. The results indicate that while the RPM is higher than that measured with the stepper motor, the torque is lower. The generator's output power depends on the magnetic field strength and the number of coils rotating within it. In this case, the torque required to rotate the generator rotor is lower than that for the stepper motor, suggesting that the generator's magnetic field is relatively weak. To enhance the output power, both RPM and torque must be increased, as indicated in Equation (2). The generator rotor is driven mechanically, which in turn determines the generator's output power. The results show that with sufficient water flow, the output power, RPM, and torque can be significantly higher than those achieved by other turbines. Therefore, it can be concluded that, provided the water flow rate is not limited, higher output power can be attained. The results presented in Table 4 indicate that the maximum output generated by the turbine is 0.231 W. Equation (1) can be used to calculate the turbine's efficiency. The net head, defined as the head available at the turbine inlet, is calculated as the difference between the head and tail levels and is also referred to as the effective head. In the hardware setup, the water pipe is buried horizontally and water is pumped from the bottom up. For this scenario, let us assume a net head of 0.01 m, a flow rate of 200 L/min, and an output power of 0.231 W. The low flow rate resulted in limited output power. According to Karunia & Ikhwali (2021), Using the same calculations, the estimated output power can be significantly higher in larger-diameter pipes. For instance, in residential areas where water capacity can reach 3000 L/s, the estimated output power is approximately 207 W. The efficiency of the proposed spherical turbine design is higher than that of the Gorlov helical turbine (cross-flow turbine), which is commonly used in residential areas of Sibu. The maximum efficiency of the Gorlov helical turbine is reported as 33.78% (Sinaga et al., 2018; Nitha et al., 2024; Carter et al., 2023). The performance of the spherical turbine was compared with that of the Gorlov helical turbine under similar flow conditions, with the spherical design demonstrating superior efficiency in confined flows. Scalability considerations, such as turbulence, sustained material wear under continuous flow, and long-term degradation in pipeline applications, were also addressed. These challenges were mitigated by selecting durable materials, such as stainless steel, and optimizing the blade geometry to maintain performance even under off-design flow conditions. According to Energy Malaysia, the average power consumption of standard streetlights is approximately 90 W (Shafie et al., 2011). Using Equation (1), the estimated power

generated by a 10-inch water pipe is 207 W, sufficient to supply energy to a streetlight. Figure 15 illustrates the portable generation system and its components, which weigh approximately 1 kg. The novelty of the spherical crossflow turbine lies in its ability to deliver locally distributed, renewable energy within urban infrastructure, such as pipeline networks. This capability is particularly significant in discussions on sustainable urban energy (Quaranta & Davies, 2022). Furthermore, the design emphasizes affordability and the potential for widespread adoption in small-scale applications, including streetlights and sensors.

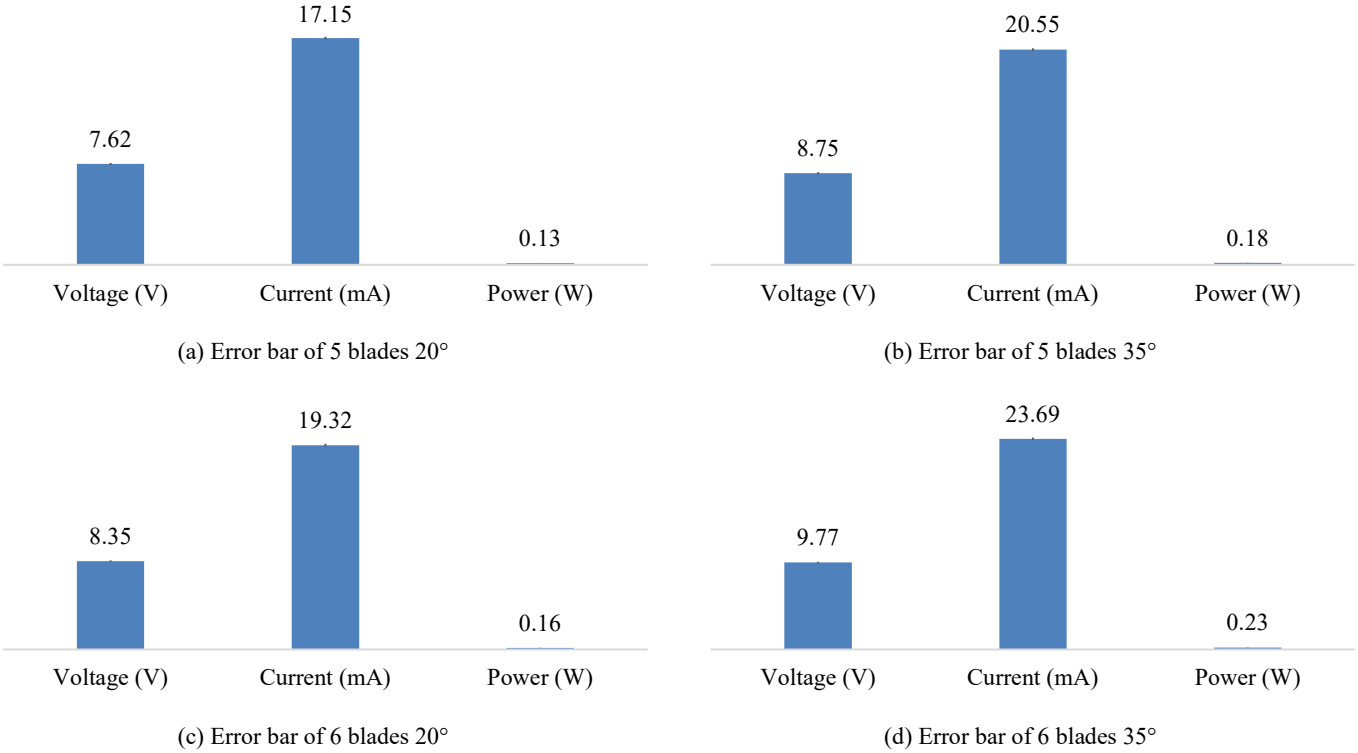


(a) Error bar of 5 blades 20°

(b) Error bar of 5 blades 35°

(c) Error bar of 6 blades 20°

(d) Error bar of 6 blades 35°

**Figure 14.** The average values for voltage, current, and power error analysis of the proposed turbines.

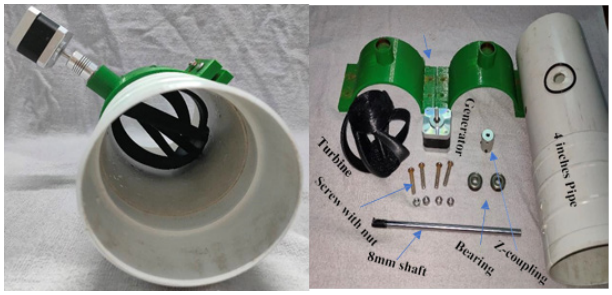


**Figure 15.** Prototype and its components.

**Table 4.** Data for the turbine with different attack angles and numbers of blades.

| First Proposed Design | | | | | | |
|---|---|---|---|---|---|---|
| **Number of blades** | **Attack angle (°)** | **Output voltage (V)** | **Output current (mA)** | **Output power (W)** | **Speed (RPM)** | **Torque (Nm)** |
| 5 | 20 | 7.62 | 17.15 | 0.131 | 239 | 0.00523 |
| 5 | 35 | 8.75 | 20.55 | 0.180 | 299-359 | 0.00575 |
| 6 | 20 | 8.35 | 19.32 | 0.161 | 299 | 0.00541 |
| 6 | 35 | 9.76 | 23.64 | 0.231 | 359 | 0.00614 |
| **Second Proposed Design** | | | | | | |
| 6 | 35 | 0 | 0 | 0 | 0 | 0 |
| First Proposed Design with Two Turbines - 6 blades 35° (Turbine 1) with 5 blades 20° (Turbine 2) | | | | | | |
| | | 8.29 | 18.98 | 0.16 | 299 | 60 |
| First Proposed Design with Two Turbines - 6 blades 35° (Turbine 1) with 5 blades 35° (Turbine 2) | | | | | | |
| | | 8.95 | 20.99 | 0.19 | 359 | 60 |
| First Proposed Design with Two Turbines - 6 blades 35° (Turbine 1) with 6 blades 20° (Turbine 2) | | | | | | |
| | | 8.00 | 18.24 | 0.15 | 299 | 0 |
| 6 blades 35° with another DC generator | | | | | | |
| 6 | 35 | 1.15 | 5.64 | 0.0065 | 538 | 0.012 m |
| Output Power by using a Driller to drive the turbine in the air | | | | | | |
| | | 38.20 | 112.30 | 4.30 | 1314 | 0.03 |

## 6. CONCLUSIONS

Significant water pressure ensures successful delivery throughout the distribution system. However, excessive pressure can damage pipes at certain points. Traditionally, pressure-reducing valves are used to lower water pressure before it reaches consumers. In this study, a portable turbine has been designed to integrate into the pipeline network, converting the kinetic energy of flowing water into usable, clean energy. This turbine can replace the pressure-reducing valve, generating free energy that can power nearby secondary applications, such as streetlights.

For further development, the strategy is to enhance the design and performance of the spherical cross-flow turbine through iterative testing and optimization. Key focus areas include exploring alternative 3D printing materials to improve durability and efficiency while accommodating a wider range of operating conditions. Another critical aspect is determining the optimal configuration of blade shape, number, and attack angle for different flow rates and pipe sizes to maximize energy harvesting. The integration of advanced sensors and real-time data collection systems will also be investigated to enable performance monitoring and adaptive control, allowing the turbine to respond dynamically to changes in water pressure. On a larger scale, this technology could be applied to distributed systems, such as municipal water treatment plants or irrigation networks, potentially reducing energy requirements and serving as a renewable power source for local communities. Further cost and feasibility analysis will be conducted to confirm the turbine's scalability and viability, with particular attention to the environmental impacts of the manufacturing process. Ultimately, this research aims to make decentralized small-scale hydropower generation accessible, affordable, and adaptable across diverse infrastructure layouts.

## 6. ACKNOWLEDGEMENT

We want to thank the School of Engineering and Technology and the University of Technology Sarawak for their support of this study.

## REFERENCES

1. Abd Rahman, I. F. S. B., & Syazwani, I. F. (2012). Design & Fabrication of Vertical Turbine for Rural Micro Hydroelectric Generation. http://utpedia.utp.edu.my/id/eprint/5578
2. Altgilbers, L. L., Grishnaev, I., Smith, I. R., Tkach, Y., Brown, M. D., Novac, B. M., & Tkach, I. (2000). Magnetocumulative generators. In Magnetocumulative Generators (pp. 57-123). Springer, New York, NY. https://doi.org/10.1007/978-1-4612-1232-4_3
3. Anand, R. S., Jawahar, C. P., Bellos, E., & Malmquist, A. (2021). A comprehensive review on Crossflow turbine for hydropower applications. Ocean Engineering, 240, 110015. https://doi.org/10.1016/j.oceaneng.2021.110015
4. Awandu, W., Ruff, R., Wiesemann, J. U., & Lehmann, B. (2022). Status of micro-hydrokinetic river technology turbines application for rural electrification in Africa. Energies, 15(23), 9004. https://doi.org/10.3390/en15239004
5. Aziz, M. S., Khan, M. A., Jamil, H., Jamil, F., Chursin, A., & Kim, D. H. (2021). Design and analysis of in-pipe hydro-turbine for an optimized nearly zero energy building. Sensors, 21(23), 8154. https://doi.org/10.2139/ssrn.3875177
6. Bachant, P., & Wosnik, M. (2015). Characterizing the near-wake of a cross-flow turbine. Journal of Turbulence, 16(4), 392-410. https://doi.org/10.1080/14685248.2014.1001852
7. Basumatary, M., Biswas, A., & Misra, R. D. (2021). Experimental verification of improved performance of Savonius turbine with a combined lift and drag based blade profile for ultra-low head river application. Sustainable Energy Technologies and Assessments, 44, 100999. https://doi.org/10.1016/j.seta.2021.100999
8. Bideris-Davos, A. A., & Vovos, P. N. (2023). Algorithm for appropriate design of hydroelectric turbines as replacements for pressure reduction valves in water distribution systems. Water, 15(3), 554. https://doi.org/10.3390/w15030554
9. Carter, J., Rahmani, A., Dibaj, M., & Akrami, M. (2023). Rainwater energy harvesting using micro-turbines in downpipes. *Energies*, *16*(4), 1660. https://doi.org/10.3390/en16041660
10. Coronado-Hernández, O. E., Fuertes-Miquel, V. S., Besharat, M., & Ramos, H. M. (2017). Experimental and numerical analysis of a water emptying pipeline using different air valves. Water, 9(2), 98. https://doi.org/10.3390/w9020098
11. Das, D., Das, S. K., Parhi, P. K., Dan, A. K., Mishra, S., & Misra, P. K. (2021). Green strategies in formulating, stabilizing and pipeline transportation of coal water slurry in the framework of WATER-ENERGY NEXUS: a state of the art review. Energy Nexus, 4, 100025. https://doi.org/10.1016/j.nexus.2021.100025
12. Ehya, H., & Faiz, J. (2022). Electromagnetic analysis and condition monitoring of synchronous generators. https://doi.org/10.1002/9781119636151
13. Espina-Valdés, R., Gharib-Yosry, A., Ferraiuolo, R., Fernández-Jiménez, A., & Fernández-Pacheco, V. M. (2022). Experimental comparison between hydrokinetic turbines: Darrieus vs. Gorlov. Environmental Sciences Proceedings, 21(1), 26. https://doi.org/10.3390/environsciproc2022021026
14. Etemadeasl, V., Esmaelnajad, R., Gharlai, K., & Riasi, A. (2024). Application of Entropy Production Theory for Evaluating the Performance of a Gorlov Hydrokinetic Turbine. Iranian Journal of Science and Technology, Transactions of Mechanical Engineering, 1-20. https://doi.org/10.1007/s40997-024-00803-9
15. Ghorbanian, V., Karney, B., & Guo, Y. (2016). Pressure standards in water distribution systems: reflection on current practice with consideration of some unresolved issues. Journal of Water Resources Planning and Management, 142(8), 04016023. https://doi.org/10.1061/(asce)wr.1943-5452.0000665
16. Ham, S., Adeeb, E., Lee, J. W., & Ha, H. (2024). Numerical evaluation of low-head inverted cross-flow turbine design method: A comprehensive study. Energy Conversion and Management, 311, 118521. https://doi.org/10.1016/j.enconman.2024.118521
17. Hangan, A., Chiru, C. G., Arsene, D., Czako, Z., Lisman, D. F., Mocanu, M., ... & Sebestyen, G. (2022). Advanced techniques for monitoring and management of urban water infrastructures—An overview. *Water*, *14*(14), 2174. https://doi.org/10.3390/w14142174
18. Hamzah, I., Prasetyo, A., Tjahjana, D. P., & Hadi, S. (2018). Effect of blade number on performance of Savonius water turbine in water pipe. In AIP conference proceedings (Vol. 1931, No. 1, p. 030046). AIP Publishing LLC. https://doi.org/10.1063/1.5024105
19. Itani, Y., Soliman, M. R., & Kahil, M. (2020). Recovering energy by hydro-turbine application in water transmission pipelines: A case study west of Saudi Arabia. Energy, 211, 118613. https://doi.org/10.1016/j.energy.2020.118613
20. Howey, D. A., Bansal, A., & Holmes, A. S. (2011). Design and performance of a centimetre-scale shrouded wind turbine for energy harvesting. Smart Materials and Structures, 20(8), 085021. https://doi.org/10.1088/0964-1726/20/8/085021
21. Hwang, J., & Kim, S. (2024). A Case Study on Sustainable Energy Use from Ballast Water Management System in Transport Vessels. Tehnički vjesnik, 31(5), 1680-1688. https://doi.org/10.17559/tv-20231012001019
22. Ibrahim, M. I., Legaz, M. J., Banawan, A. A., & Ahmed, T. M. (2025). CFD Design Optimisation for the Hydrodynamic Performance of the Novel Fin-Ring Horizontal Axis Hydrokinetic Turbine. Journal of Marine Science & Engineering, 13(2). https://doi.org/10.3390/jmse13020323
23. Jayaram, V., & Bavanish, B. (2022). Design and analysis of gorlov helical hydro turbine on index of revolution. International Journal of Hydrogen Energy, 47(77), 32804-32821. https://doi.org/10.1016/j.ijhydene.2022.07.181
24. Jilani, A., & Razali, A. (2018). Centrifugal Pump Performance Characteristics for Domestic Application. In MATEC Web of Conferences (Vol. 225, p. 05011). EDP Sciences. https://doi.org/10.1051/matecconf/201822505011
25. Kamal, M. M., & Saini, R. P. (2022). A review on modifications and performance assessment techniques in cross-flow hydrokinetic system.

Sustainable Energy Technologies and Assessments, 51, 101933. https://doi.org/10.1016/j.seta.2021.101933

26. Kamoji, M. A., Kedare, S. B., & Prabhu, S. V. (2009). Performance tests on helical Savonius rotors. Renewable Energy, 34(3), 521-529. https://doi.org/10.1016/j.renene.2008.06.002
27. Karunia, T. U., & Ikhwali, M. F. (2021). Effects of population and land-use change on water balance in DKI Jakarta. In IOP Conference Series: Earth and Environmental Science (Vol. 622, No. 1, p. 012045). IOP Publishing. https://doi.org/10.1088/1755-1315/622/1/012045
28. Khalid, M. R. W., Reza K. K., & Ghorbani, S. (2023). Common Failures in Hydraulic Kaplan Turbine Blades and Practical Solutions. Materials, 16(9), 3303. https://doi.org/10.3390/ma16093303
29. Kirke, B. (2024). Towards more cost-effective river hydrokinetic turbines. Energy for Sustainable Development, 78, 101370. https://doi.org/10.1016/j.esd.2023.101370
30. Kumar, K., & Saini, R. P. (2022). Economic analysis of operation and maintenance costs of hydropower plants. Sustainable Energy Technologies and Assessments, 53, 102704. https://doi.org/10.1016/j.seta.2022.102704
31. Mamassis, N., Efstratiadis, A., Dimitriadis, P., Iliopoulou, T., Ioannidis, R., & Koutsoyiannis, D. (2021). Water and Energy. Handbook of Water Resources Management: Discourses, Concepts and Examples, 619–657. https://doi.org/10.1007/978-3-030-60147-8_20
32. Miao, G., Fang, S., Wang, S., & Zhou, S. (2022). A low-frequency rotational electromagnetic energy harvester using a magnetic plucking mechanism. Applied Energy, 305, 117838. https://doi.org/10.1016/j.apenergy.2021.117838
33. Mosbahi, M., Ayadi, A., Mabrouki, I., Driss, Z., Tucciarelli, T., & Abid, M. S. (2019). Effect of the converging pipe on the performance of a lucid spherical rotor. Arabian Journal for Science and Engineering, 44(2), 1583-1600. https://doi.org/10.1007/s13369-018-3625-0
34. Mosbahi, M., Ghodhbani, D., Derbel, M., & Driss, Z. (2022). Performance study of a lucid spherical rotor. In Advances in Mechanical Engineering and Mechanics II: Selected Papers from the 5th Tunisian Congress on Mechanics, CoTuMe 2021, March 22–24, 2021 (pp. 451-457). Springer International Publishing. https://doi.org/10.1007/978-3-030-86446-0_59
35. Musa, M., Ghobrial, L., Sasthav, C., Heineman, J., Rencheck, M., Stewart, K., DeNeale, S., Tseng, C.-Y., White, D., Davis, L., Nachman, M., & Kelsey, R. (2023). Advanced Manufacturing and Materials for Hydropower: Challenges and Opportunities. Office of Scientific and Technical Information (OSTI). https://doi.org/10.2172/1960692
36. Mutlu, Y., & Çakan, M. (2018). Evaluation of in-pipe turbine performance for turbo solenoid valve system. Engineering Applications of Computational Fluid Mechanics, 12(1), 625-634. https://doi.org/10.1080/19942060.2018.1506364
37. Nitha, N., Pasa, N., Fikran, F., Bontong, Y., & Sampelawang, P. (2024). Efisiensi Turbin Air Gorlov Empat Sudu Helical dengan Variasi Pitch Angle. Innovative: Journal Of Social Science Research, 4(3), 19091-19101. https://j-innovative.org/index.php/Innovative/article/view/15325
38. Ong, C. S. (2011). Prototype of an efficient hyrdopower plant (Doctoral dissertation, UTAR). http://eprints.utar.edu.my/149/1/MH-2011-0703227-1.pdf
39. Pranio, J., & Karnowo, K. (2019). The Effect Of Blade Number And Water Velocity Toward The Performance Of Heliks Gorlov Turbine. Jurnal Penelitian Saintek, 24(2), 108-120. https://doi.org/10.21831/jps.v24i2.20287
40. Quaranta, E., & Davies, P. (2022). Emerging and innovative materials for hydropower engineering applications: Turbines, bearings, sealing, dams and waterways, and ocean power. Engineering, 8, 148-158. https://doi.org/10.1016/j.eng.2021.06.025
41. Rahman, A., Farrok, O., & Haque, M. M. (2022). Environmental impact of renewable energy source based electrical power plants: Solar, wind, hydroelectric, biomass, geothermal, tidal, ocean, and osmotic. Renewable and Sustainable Energy Reviews, 161, 112279. https://doi.org/10.1016/j.rser.2022.112279
42. Reddy, K. B., Bhosale, A. C., & Saini, R. P. (2022). Performance parameters of lift-based vertical axis hydrokinetic turbines-A review. Ocean Engineering, 266, 113089. https://doi.org/10.1016/j.oceaneng.2022.113089
43. Rendi, R., Arifin, J., & Pauzan, M. (2024). Enhanced Performance of the Gorlov Hydrokinetic Turbine through Blade Profile Modification. SINTEK JURNAL: Jurnal Ilmiah Teknik Mesin, 18(1), 19–25. https://doi.org/10.24853/sintek.18.1.19-25
44. Roy, S., & Saha, U. K. (2015). Wind tunnel experiments of a newly developed two-bladed Savonius-style wind turbine. Applied Energy, 137, 117-125. https://doi.org/10.1016/j.apenergy.2014.10.022
45. Saini, G., & Saini, R. P. (2023). Clearance and blockage effects on hydrodynamic performance of hybrid hydrokinetic turbine. Sustainable Energy Technologies and Assessments, 57, 103210. https://doi.org/10.1016/j.seta.2023.103210
46. Shafie, S. M., Mahlia, T. M. I., Masjuki, H. H., & Andriyana, A. (2011). Current energy usage and sustainable energy in Malaysia: A review. Renewable and Sustainable Energy Reviews, 15(9), 4370-4377. https://doi.org/10.1016/j.rser.2011.07.113
47. Shankara Murthy, H. M., Hegde, R. N., Gaonkar, R. U., & Rai, N. (2024). A critical assessment of significant developments in wind turbine performance. International Journal of Ambient Energy, 45(1), 2267568. https://doi.org/10.1080/01430750.2023.2267568
48. Siavash, N. K., Najafi, G., Hashjin, T. T., Ghobadian, B., & Mahmoodi, E. (2020). An innovative variable shroud for micro wind turbines. Renewable Energy, 145, 1061-1072. https://doi.org/10.1016/j.renene.2019.06.098
49. Sinaga, J. B., Tanti, N., Suudi, A., & Susila, M. D. (2018). Development of a Model of Hydro Electric Power Generation Suitable for Low Head. In Journal of Physics: Conference Series (Vol. 1116, No. 3, p. 032034). IOP Publishing. https://doi.org/10.1088/1742-6596/1116/3/032034
50. Singh, V. K., & Singal, S. K. (2017). Operation of hydro power plants-a review. Renewable and Sustainable Energy Reviews, 69, 610-619. https://doi.org/10.1016/j.rser.2016.11.169
51. Skroufouta, S., & Baltas, E. (2021). Investigation of hybrid renewable energy system (HRES) for covering energy and water needs on the Island of Karpathos in Aegean Sea. Renewable Energy, 173, 141–150. https://doi.org/10.1016/j.renene.2021.03.113
52. Strielkowski, W., Civín, L., Tarkhanova, E., Tvaronavičienė, M., & Petrenko, Y. (2021). Renewable Energy in the Sustainable Development of Electrical Power Sector: A Review. Energies, 14(24), 8240. https://doi.org/10.3390/en14248240
53. Timmis, H. (2021). Modeling with Fusion 360. In Practical Arduino Engineering: End to End Development with the Arduino, Fusion 360, 3D Printing, and Eagle (pp. 57-127). Berkeley, CA: Apress. https://doi.org/10.1007/978-1-4842-6852-0_3
54. Tu, L. T., Phap, V. M., & Huong, N. T. T. (2023). A study on loan repayment options for power plant construction: a case study of the Son La hydropower plant, Vietnam. Polityka Energetyczna – Energy Policy Journal, 26(2), 121–140. https://doi.org/10.33223/epj/163506
55. Umar, D. A., Yaw, C. T., Koh, S. P., Tiong, S. K., Alkahtani, A. A., & Yusaf, T. (2022). Design and optimization of a small-scale horizontal-axis wind turbine blade for energy harvesting at low wind profile areas. Energies, 15(9), 3033. https://doi.org/10.3390/en15093033
56. University of Aberdeen. (2023). A comparative analysis of hydrokinetic turbine performance at low Reynolds numbers. Elsevier Pure. Retrieved from https://abdn.elsevierpure.com/en/publications/a-comparative-analysis-of-hydrokinetic-turbine-performance-at-low
57. Vijayan, J., & Retnam, B. B. (2022). A Brief Study on the Implementation of Helical Cross-Flow Hydrokinetic Turbines for Small Scale Power Generation in the Indian SHP Sector. International Journal of Renewable Energy Development, 11(3). https://doi.org/10.14710/ijred.2022.45249
58. Walker, S. R. J., & Thies, P. R. (2022). A life cycle assessment comparison of materials for a tidal stream turbine blade. Applied Energy, 309, 118353. https://doi.org/10.1016/j.apenergy.2021.118353
59. Whitby, R. D. (2021). Lubricant Condition Monitoring Programmes, Their Implementation, Benefits and How to Avoid Problems. Lubricant Analysis and Condition Monitoring, 353–368. https://doi.org/10.1201/9781003245254-16
60. Williams, A. (2003). Pumps as turbines: a user's guide. ITDG Pub. https://www.google.com/books/edition/Pumps_as_Turbines/KPpSAAAAMAAJ?hl=en
61. Yavuz, T., & Koç, E. (2012). Performance analysis of double blade airfoil for hydrokinetic turbine applications. Energy conversion and management, 63, 95-100. https://doi.org/10.1016/j.enconman.2012.01.032
62. Yazdi, M. (2024). Maintenance Strategies and Optimization Techniques. Advances in Computational Mathematics for Industrial System Reliability and Maintainability, 43–58. https://doi.org/10.1007/978-3-031-53514-7_3